Springer

KSME

Journal of Mechanical Science and Technology 32 (3) (2018) 1333~1344
www.springerlink.com/content/1738-494x(Print)/1976-3824(Online)
DOI 10.1007/s12206-018-0237-2

Mobility properties analyses of a wall climbing hexapod robot †

Bin He[1,*], Shoulin Xu[1], Yanmin Zhou[1] and Zhipeng Wang[2]

[1]*Department of Control Science and Engineering, Tongji University, Shanghai, 201804, China*
[2]*School of Mechanical Engineering, Tongji University, Shanghai, 201804, China*

(Manuscript Received May 5, 2017; Revised October 12, 2017; Accepted December 12, 2017)

Abstract

In this paper, we investigate the Degree of freedom (DOF), workspace and singularity of a wall climbing hexapod robot. The robot has two typical working modes, which are the six or three legs attaching on the wall, so robot can be regarded as 6SRRR or 3SRRR parallel mechanism, respectively. First, the DOF of the robot is analyzed by the screw theory. The result indicates that two configurations of the robot possess 6-DOF, and the screw theory makes the calculation of the DOF become extremely simple. Moreover, the workspace of the robot body is studied with constraint equations, which obtains the influence of structural parameters on workspace. After that, a new simple Jacobian matrix is proposed to analyze the singularity, and obtain the singular configurations of the robot, which greatly simplifies the calculation of Jacobian matrix of the robot. Finally, by experiments to verify that the singularity analysis method is correct. The singularity analysis of this paper could be applied for effective control of the robot to avoid singular configurations.

Keywords: Wall climbing hexapod robot; Screw theory; Degree of freedom; Constraint equations; Workspace; Singularity

1. Introduction

For lighting and aesthetic considerations, glass curtain walls are often used in on high buildings in modern cities. Due to the perennial exposure in the air, contaminations accumulate on the glass curtain wall, which needs to be cleaned and maintained regularly. At present, cleaning these glass walls is mainly done manually by cleaners using ropes or hanging baskets. These cleaners need to work in really hard environment, with high intensity of labor, at great risk but still low efficiency. The development of the robot technology provides a better alternative for the glass wall cleaning to improve the working environment of workers, and reduce the cost, etc.

The research of wall cleaning robots mainly includes: The cleaning device, the integration of the robot and the cleaning device, and the wall climbing robot with attachment and motion function, which is one of the most critical contents. At present, the main attachment ways of the wall climbing robot include: magnetic adhesion [1], adhesion of adhesive materials [2] and vacuum adhesion [3]. Each of these adhesion mechanisms has advantages and drawbacks. The mechanism of the magnetic adhesion is simple, but its application is limited on surfaces of permeability magnetic material. Adhesion of adhesive materials can be applied to wall surfaces of any shape and material, but this method is hard to be applied to large size robots. Since glass curtain walls are considered as a cleaning object in this paper. The vacuum adhesion can be very strong and has wide application potentials in glass curtain walls, so robot uses vacuum adhesion in this paper. The motion ways of the wall climbing robot mainly include: Crawler-type [4], frame type [5], wheeled type [6] and legged type [7]. The crawler-type robots can achieve high movement speed, but are difficult in terms of changing the movement direction. The frame type robot's control and work are simple and convenient, but its movements are not continuous and are slow. The structure of a wheeled type robot is simple and the movement speed is high, but the obstacle crossing ability is weak. Legged type robots can be applied on different wall surfaces, and they have strong obstacle crossing abilities.

Among legged robots, when the robot is walking, the stability of hexapod robots is stronger than biped robots and quadruped robots, and the control of hexapod robots is simpler than the eight legged robots. Osaka University in Japan developed a hexapod robot called ASTERISK, each leg of which possessed 4 joints. The robot could climb a vertical ladder by the hook design at each foot end [8]. Wang [9] investigated motion performance of a radial symmetrical six-legged robot. García-López [10] researched trajectory generation in one leg of a hexapod robot. Zhang [11] analyzed a bionic hexapod robot for walking on unstructured terrain. In order to develop a robot to meet these requirements of glass curtain wall cleaning, through the above analysis, we use a hexapod robot aided

*Corresponding author. Tel.: +86 18621116388, Fax.: +86 18621116388
E-mail address: hebin@tongji.edu.cn
† Recommended by Associate Editor Baek-Kyu Cho
© KSME & Springer 2018

by the vacuum adhesion as a carrier for the cleaning devices.

When the wall climbing hexapod robot adheres on a wall, it can be seen as a parallel mechanism. It has the advantages of high rigidity, high flexibility, high precision, long service life, good power performance [12], easy control etc. DOF is an important research content of mechanisms, because it is the premise of realizing a motion of a robot. Gan [13] studied constraint based limb synthesis and mobility change aimed mechanism construction. Kong [14] investigated 3 DOF spherical parallel manipulators by screw theory. Dai [15] studied mobility of an overconstrained parallel mechanism. Bu [16] analyzed mobility of parallel manipulators based on intersection of screw manifolds.

For engineering applications, the workspace of the end actuator is one of the most concerned problems of research, since it affects the work efficiency to complete the task of the robot. Many scholars had studied the position of positive and inverse solutions and workspace of the end actuator of space parallel mechanisms [17]. For solving the workspace of parallel machines, Wang [18] studied the boundary search algorithm. Gao [19] analyzed the inverse kinematics and workspace of a metamorphic hand. Agheli [20] presented a general methodology for solving the closed-form constant orientation workspace of radially symmetric hexapod robots. Szep [21] analyzed the workspace of a Delta parallel robot. Maldonado-Echegoyen [22] studied a 3DOF translational parallel robot for drilling tasks based on two 5-bar mechanisms with a large workspace.

During walking, there are problems of singularity in the workspace of a robot. Once a mechanical system works at a singular position, its DOF may change, including the number, type and direction, which may cause the instability of walking and attachment. The singular configuration of a mechanism can be obtained by analyzing the condition when the Jacobi's determinant is equal to zero, which is called matrix method. Gosselin divided the singular configuration of a parallel mechanism into three forms: the boundary singularity, the local singularity and the structure singularity [23]. Merlet analyzed the singularity of the mechanism by using the Grassmann method [24]. Many researchers studied the singularity of the mechanism with the screw theory [25]. Gan [26] studied forward displacement of 1CCC-5SPS parallel mechanism by Grobner theory. Zarkandi [27] analyzed singularity of a parallel mechanism with three revolute joints and a prismatic joint. Zhao [28] investigated mobility properties of Schoenflies-type parallel manipulator by Jacobian matrix of constraint equation.

In this paper, the main contribution is to develop a new wall climbing hexapod robot, and investigates the DOF, workspace and singularity of the wall climbing hexapod robot. The paper is organized as follows. In Sec. 2, the robot has two kinds of configurations relating to its attachment on a vertical wall with six or three feet, which can be regarded as a 6SRRR and 3SRRR parallel mechanism, therefore, we investigate the DOF of the robot by the screw theory, respectively. In Sec. 3, the workspaces of these two configurations were analyzed through constraint equations, obtaining the influence of structure parameters of leg on workspace. In Sec. 4, the previous studies of Jacobian matrix of parallel mechanisms, which mainly reflect the relationship between the output independent variables and input independent variables. However, solving process is very complicated. Thus, we present a simple method to calculate the Jacobi matrix, and obtain the singular configurations of the robot. In Sec. 5, the experiments are used to show that the singularity analysis of the robot is correct. This paper provides a guidance for stable performance control of the robot climbing on the wall.

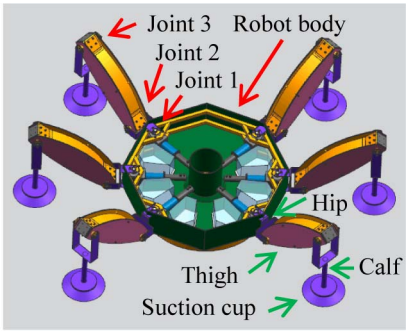

Fig. 1. The CAD model of the wall climbing hexapod robot.

2. Mechanism screw system and mobility analysis

In this section, we first design a wall climbing hexapod robot, the CAD model is shown in Fig. 1. The body frame of the robot is in a shape of regular octagon and installed with the communication, control, energy, and other circuit systems and the cleaning or repairing equipment. The robot is designed with six legs and each of which consists of four components: The suction cup, calf, thigh and hip. The suction cup and calf are connected by a spherical joint; while the calf and the thigh, the thigh and the hip are connected by revolute joints, which are parallel to the body. The hip and the body are also connected via a revolute joint, but is perpendicular to the body. The connection between calf and thigh is defined as Joint 3, the connection between thigh and hip is defined as Joint 2, the connection between hip and body is defined as Joint 1. The suction cup provides a negative pressure, which generates the adhesive force that makes the robot adhere on the vertical glass curtain wall. The robot's structure, when climbing on a vertical wall, stays the same as in the horizontal plane. Therefore the study of the DOF of the robot in the vertical plane could be easily performed in the horizontal plane. A mathematical model of the robot frame is shown in Fig. 2 to facilitate the expressing of the screw system of the robot. Points of A_1, A_2, A_3, A_4, A_5 and A_6 are the contact point between the six feet and the wall, and the length of A_2A_5 is $2R$. Points of D_1, D_2, D_3, D_4, D_5 and D_6 are the connecting point between the legs and the robot body, and the length of D_2D_5 is $2r$. The plane of $A_1A_2A_3A_4A_5A_6$ forms the base plane,

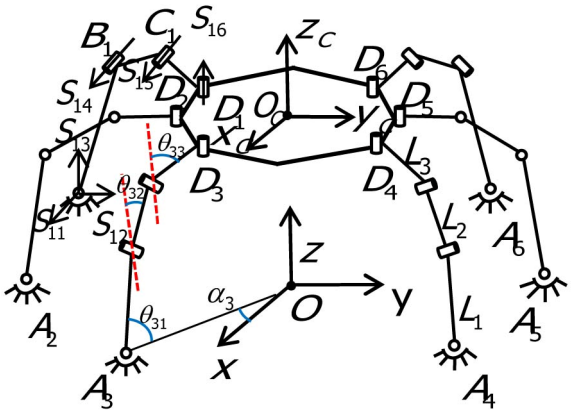

Fig. 2. The mathematical model of the wall climbing hexapod robot.

while $D_1 D_2 D_3 D_4 D_5 D_6$ forms the body plane of the robot. The geometrical center of the regular octagon is defined as point O, which is the origin of the coordinate system. The axis of y lies in the direction of $A_2 A_5$; z is perpendicular to the plane of Oxy and points from the base to the body plane of the robot; and x is then defined according to the right-hand rule together with y and z. $A_i (i = 1,2,3,4,5,6)$ presents the spherical joint, and B_i, C_1 and D_i are revolute joints. The length of the calf, thigh and hip are L_1, L_2 and L_3. The angle of $\theta_{i1} (0° \le \theta_{i1} \le 90°)$ is defined as the angle between $A_i B_i$ and the projection of $A_i B_i$ in Oxy plane; $\alpha_i (0° \le \alpha_i \le 90°)$ is that between the axis of x and the projection of $A_i B_i$ in the Oxy plane; $\theta_{i2} (0° \le \theta_{i2} \le 90°)$ is that between line $B_i C_i$ and the axis of z; and $\theta_{i3} (0° \le \theta_{i3} \le 180°)$ is the angle between line $C_i D_i$ and the axis of z. The leg $A_i B_i C_i D_i$ is defined as the i th leg.

The symbol S is defined as a screw which is a 6 dimensional linear vector space. It can be expressed as following:

$$S = \left[S_0, r \times S_0 + h S_0 \right] = \left[L, M, N, P, Q, R \right] \tag{1}$$

where $S_0 = [L, M, N]$ denotes the unit vector along the screw axis, $r \times S_0 + h S_0 = [P, Q, R]$ expresses the moment part of the screw, the vector r denotes any point on the screw axis, and h is the pitch of the screw. For a revolute joint, $h = 0$. Its screw can therefore be represented in $S_r = [S_0, r \times S_0]$. For a prismatic joint, its screw can be represented as $S_r = [0, S_0]$. As to the motion screws, the rotation about the screw axis is indicated in the first three components, while the translation along the screw axis is expressed in the remaining three components. Regarding to the constraint screws, the force along the screw axis is denoted by the first three components and the torque in the last three components [25, 29].

The branch motion screw system of each leg was analyzed based on the mathematical model shown in Fig. 2. $S_{ij} (i = 1, 2, 3, 4, 5, 6;\ j = 1, 2, 3, 4, 5, 6)$ is defined as the screw of the j th joint in the i th leg. The spherical joints of each leg consist of S_{i1}, S_{i2} and S_{i3}. The revolute joints at points B_i, C_1 and D_i generate S_{i4}, S_{i5} and S_{i6}, respectively. In order to simplify the expression, we define the following formula in the full text.

$$\begin{cases} s\alpha_1 = \sin\alpha_1 \\ c\alpha_1 = \cos\alpha_2 \\ n_2 = \sin\alpha_1 + \cos\alpha_1 \end{cases} \tag{2}$$

$$\begin{cases} g_1 = L_1 \cos\theta_{11} + L_2 \sin\theta_{12} \\ d_2 = (L_1 \sin\theta_{11} + L_2 \cos\theta_{12}) \cos\alpha_1 \\ e_1 = (L_1 \sin\theta_{11} + L_2 \cos\theta_{12}) \sin\alpha_1 \end{cases} \tag{3}$$

$$\begin{cases} p_1 = L_1 \sin\alpha_1 \sin(\theta_{11} + \theta_{13}) \\ \quad + L_2 \sin\alpha_1 \cos(\theta_{12} - \theta_{13}) + L_3 \sin\alpha_1 \\ q_1 = L_1 \cos\alpha_1 \sin(\theta_{11} + \theta_{13}) \\ \quad + L_2 \cos\alpha_1 \cos(\theta_{12} - \theta_{13}) + L_3 \cos\alpha_1 . \end{cases} \tag{4}$$

Here, supposing that the $\{S_{bi}]$ is motion-screw system of the leg $i (i = 1, 2, 3, 4, 5, 6)$, and the form such as $\{S_{bi}\} = \{S_{i1}, S_{i2}, S_{i3}, S_{i4}, S_{i5}, S_{i6}\}$. Based on the symbols defined above, the branch motion-screw systems of leg 1 can be expressed in the coordinate system of $O - xyz$ as following:

$$\begin{aligned} &\{S_{b1}\} = \\ &S_{11} = \left(1, 0, 0, 0, 0, \frac{\sqrt{2}}{2} R \right)^T \\ &S_{12} = \left(0, 1, 0, 0, 0, -\frac{\sqrt{2}}{2} R \right)^T \\ &S_{13} = \left(0, 0, 1, -\frac{\sqrt{2}}{2} R, \frac{\sqrt{2}}{2} R, 0 \right)^T \\ &S_{14} = \left(s\alpha_1, -c\alpha_1, 0, L_1 s\theta_{11} c\alpha_1, L_1 s\theta_{11} s\alpha_1, \right. \\ &\qquad \left. \frac{\sqrt{2}}{2} R n_1 - L_1 c\theta_{11} \right)^T \\ &S_{15} = \left(s\alpha_1, -c\alpha_1, 0, d_1, e_1, \frac{\sqrt{2}}{2} R n_1 - g_1 \right)^T \\ &S_{16} = \left(-c\theta_{13} c\alpha_1, -c\theta_{13} s\alpha_1, s\theta_{13}, -\frac{\sqrt{2}}{2} R s\theta_{13} + p_1, \right. \\ &\qquad \left. \frac{\sqrt{2}}{2} R s\theta_{13} - q_1, \frac{\sqrt{2}}{2} R n_1 c\theta_{13} \right)^T . \end{aligned} \tag{5}$$

It can be calculated that, each vector in this screw system $\{S_{b1}\}$ is linearly independent. Since the linear correlation of vector is independent of the choice of the coordinate system, the screw systems of legs 1, 2, 3, 4, 5 and 6 are all the screw six-system. It is supposed that $\{S_{bi}^r\} (i = 1, 2, 3, 4, 5, 6)$ is the constraint screw system of $\{S_{bi}\}$. According to the reciprocal product equation, that is $\{S_{bi}^T\} \Delta \{S_{bi}^r\} = 0$, where $\Delta = \begin{bmatrix} 0 & J \\ J & 0 \end{bmatrix}$

with the identity matrix I. It is obvious that all of these branch constraint-screw systems $\{S_{bi}^r\}$ are all screw zero-system. If $\{S^r\}$ is defined as the platform constraint-screw systems, then the following equation can then be obtained

$$\{S^r\} = \sum_{i=1}^{6} \{S_{bi}^r\} . \tag{6}$$

The motion-screw of the platform is determined by the reciprocal of the platform constraint-screw system. If $\{S^f\}$ is defined as the motion-screw of the platform, the reciprocal product equation $\{S^f\} \circ \{S^r\} = 0$, since $\{S^r\}$ is a screw zero-system. It is then can be obtained that $\{S^f\}$ is the screw six-system.

A conclusion can therefore be drawn that the platform $D_1 D_2 D_3 D_4 D_5 D_6$ has 6-DOF. When the six feet of robot adhere on the wall, the robot body can achieve three directions of translation and three directions of rotation along and around the x, y and z-axis, respectively.

During robot walking with triangle gait on a vertical wall, the robot lifts its 2nd, 4th and 6th legs simultaneously when employs the 1st, 3rd and 5th legs to adhere on the wall, and *vice versa*. Same analyzing methods as introduced above also apply for the mobility study in this situation. It can be obtained that the robot body also has 6-DOF when it attaches on a wall with three legs, meaning that the body can fulfill three directions of translation and three directions of rotation along and around the x, y and z-axis, respectively.

In the above, we analyze the DOF of the two special configurations with screw theory. The linear correlation and linear independence between vectors are independent of the choice of the different coordinate system, the screw system of each leg is the screw six-system in the coordinate system $O - xyz$, thus, the screw system of each leg is the screw six-system in any coordinate system. It can be obtained that, no matter where the robot adheres on a wall with six feet, the robot body has 6-DOF. In the same way, no matter where the robot adheres on a wall with three feet, the robot body can achieve the flexible motion with 6-DOF. Namely, the robot body can realize three directions of translation and three directions of rotation in the space no matter where the robot adheres on a wall with six or three feet. The robot body can achieve the flexible motion with 6-DOF, and can be used as a carrier platform that provides motion with 6-DOF to the corresponding mechanism.

3. Analysis of workspace

In the above section, we obtained that the robot body has 6-DOF, thus explained that the body can realize motion in the space. Here, we study the workspace of the robot body. The workspace of the wall climbing hexapod robot influences the stride length of the robot. When the robot attaches on a wall with six legs, it can be seen as a 6SRRR parallel mechanism; while it can be regarded as a 3SRRR parallel mechanism during the walking with triangle gait using three legs to adhere on the wall. The workspaces of the robot for these two working modes are studied.

The robot is mainly used to clean the vertical glass wall, in order to ensure the effective cleaning on the wall, the robot body is required to be parallel to the wall. Therefore, the studies are limited to the body postures that are parallel to the vertical wall. Next, we study the motion of the robot body along the x, y and z-axis and rotation around the z-axis, regardless of its number of adhering legs (Six or three).

We firstly introduce the workspace of the robot adhering on the wall with six legs. Since only consider the motion of the robot body along the x, y and z-axis and rotation around the z-axis, four independent variables are needed to establish the constraint equations of the workspace. The (x, y, z) is used to define the reference point of absolute coordinates of the geometric center C of the body; while α is the angle variable. So the transformation matrix from the local to the absolute coordinate system can be expressed as

$$R_1 = \begin{bmatrix} \cos\alpha & -\sin\alpha & 0 \\ \sin\alpha & \cos\alpha & 0 \\ 0 & 0 & 1 \end{bmatrix} . \tag{7}$$

It is supposed that the robot body is also in a regular octagon shape with point C as its geometric center. $O_C - x_C y_C z_C$ is the local coordinate system with its coordinate origin at point C; the axis of y_C points in the direction of $D_2 D_5$; z_C is perpendicular to the plane of $O_C x_C y_C$ pointing from the base to the body of the robot; and x_C is defined according to the right-hand rule, as shown in Fig. 2. In order to make the workspace is not an empty set, we assume $L_1 + L_2 + L_3 + r > R$ and $r + L_3 < R$. In the local coordinate system, the coordinates of these six vertices of the body are given as

$$\begin{cases} D_1^L\left(-\dfrac{\sqrt{2}}{2}r, -\dfrac{\sqrt{2}}{2}r, 0\right), D_2^L(0, -r, 0), \\ D_3^L\left(\dfrac{\sqrt{2}}{2}r, -\dfrac{\sqrt{2}}{2}r, 0\right), D_4^L\left(\dfrac{\sqrt{2}}{2}r, \dfrac{\sqrt{2}}{2}r, 0\right), \\ D_5^L(0, r, 0), D_6^L\left(-\dfrac{\sqrt{2}}{2}r, -\dfrac{\sqrt{2}}{2}r, 0\right). \end{cases} \tag{8}$$

If $D_1^L(x_{D_1}^L, y_{D_1}^L, z_{D_1}^L)$ is the local coordinates of point $i (i = 1, 2, 3, 4, 5, 6)$ and $D_i(x_{D_1}, y_{D_1}, z_{D_1})$ is the absolute coordinates of point i, the following equation can be obtained that

$$\begin{bmatrix} x_{D_1} \\ y_{D_1} \\ z_{D_1} \end{bmatrix} = \begin{bmatrix} x \\ y \\ z \end{bmatrix} + R_1 \begin{bmatrix} x_{D_1}^L \\ y_{D_1}^L \\ z_{D_1}^L \end{bmatrix} = \begin{bmatrix} x + x_{D_1}^L \cos\alpha - y_{D_1}^L \sin\alpha \\ y + x_{D_1}^L \sin\alpha + y_{D_1}^L \cos\alpha \\ z + z_{D_1}^L \end{bmatrix} . \tag{9}$$

In the absolute coordinate system, by operation of vector addition, the following equation can be established for each leg

$$\overrightarrow{OC_i} = \overrightarrow{OAC_i} + \overrightarrow{A_iB_i} + \overrightarrow{B_iC_i} . \tag{10}$$

In order to simplify the expression, we define the following formula in the full text.

$$\begin{cases} n = \sin\alpha + \cos\alpha \\ u = \sin\alpha - \cos\alpha \end{cases} \tag{11}$$

$$\begin{cases} h_i = L_1 \sin\theta_{i1} + L_2 \cos\theta_{i2} \\ b_i = (L_1 \cos\theta_{i1} + L_2 \sin\theta_{i2}) \cos\alpha_1 \\ v_i = (L_1 \cos\theta_{i1} + L_2 \sin\theta_{i2}) \sin\alpha_i \end{cases} \tag{12}$$

where $i = 1, 2, 3, 4, 5, 6$.

Through the operation of the coordinates, the following formula can then be achieved

$$\begin{cases} \overrightarrow{OC_1} = \left(-\left(\dfrac{\sqrt{2}}{2} R - b_1 \right), -\left(\dfrac{\sqrt{2}}{2} R - v_1 \right), h_1 \right)^T \\ \overrightarrow{OC_2} = (b_2, -(R - v_2), h_2)^T \\ \overrightarrow{OC_3} = \left(\dfrac{\sqrt{2}}{2} R + b_3, -\left(\dfrac{\sqrt{2}}{2} R - v_3 \right), h_3 \right)^T \\ \overrightarrow{OC_4} = \left(\dfrac{\sqrt{2}}{2} R + b_4, \dfrac{\sqrt{2}}{2} R - v_4, h_4 \right)^T \\ \overrightarrow{OC_5} = (b_5, R - v_5, h_5)^T \\ \overrightarrow{OC_6} = \left(-\left(\dfrac{\sqrt{2}}{2} R - b_6 \right), \dfrac{\sqrt{2}}{2} R - v_6, h_6 \right)^T . \end{cases} \tag{13}$$

By the addition and subtraction of vector, the following equation can be obtained

$$\begin{cases} \overrightarrow{OD_i} = \overrightarrow{OC} + \overrightarrow{CD_i} \\ \overrightarrow{C_iD_i} = \overrightarrow{OD_i} - \overrightarrow{OC_1} . \end{cases} \tag{14}$$

The constraint equation of leg $i (i = 1, 2, 3, 4, 5, 6)$ can be obtained in the following form

$$\left\| \overrightarrow{C_iD_i} \right\|^2 - L_3^2 = 0 . \tag{15}$$

In order to represent the workspace of the robot, expanding Eq. (15), the constraint equation can be expressed as

$$F(x, y, z, \alpha) = \begin{bmatrix} f_1 \\ f_2 \\ f_3 \\ f_4 \\ f_5 \\ f_6 \end{bmatrix} \tag{16}$$

where

$$\begin{cases} f_1 = \left(x + \dfrac{\sqrt{2}}{2} ru + \dfrac{\sqrt{2}}{2} R - b_1 \right)^2 + \left(y - \dfrac{\sqrt{2}}{2} rn + \dfrac{\sqrt{2}}{2} R - v_1 \right)^2 + (z - h_1)^2 - L_3^2 \\ f_2 = (x + rs\alpha - b_2)^2 + (y - rc\alpha + R - v_2)^2 + (z - h_2)^2 - L_3^2 \\ f_3 = \left(x + \dfrac{\sqrt{2}}{2} rn - \dfrac{\sqrt{2}}{2} R - b_3 \right)^2 + \left(y + \dfrac{\sqrt{2}}{2} ru + \dfrac{\sqrt{2}}{2} R - v_3 \right)^2 + (z - h_3)^2 - L_3^2 \\ f_4 = \left(x - \dfrac{\sqrt{2}}{2} ru - \dfrac{\sqrt{2}}{2} R - b_4 \right)^2 + \left(y + \dfrac{\sqrt{2}}{2} rn - \dfrac{\sqrt{2}}{2} R + v_4 \right)^2 + (z - h_4)^2 - L_3^2 \\ f_5 = (x - rs\alpha - b_5)^2 + (y + rc\alpha - R + v_5)^2 + (z - h_5)^2 - L_3^2 \\ f_6 = \left(x - \dfrac{\sqrt{2}}{2} rn + \dfrac{\sqrt{2}}{2} R - b_6 \right)^2 + \left(y - \dfrac{\sqrt{2}}{2} ru - \dfrac{\sqrt{2}}{2} R + v_6 \right)^2 + (z - h_6)^2 - L_3^2 . \end{cases} \tag{17}$$

The workspace of the robot body is indicated as

$$W_R = \left\{ (x, y, z, \alpha) \middle| F(x, y, z, \alpha) = 0 \right\} \tag{18}$$

where 0 is a 6x1 matrix. Equation $F(x, y, z, \alpha)$ is the constraint equation of the geometric center C of the body.

It can be seen from Eq. (18) that the range of the spherical center coordinate as well as the workspace of the robot body increases with L_1, L_2 and L_3, indicating that the length of the calf, thigh and hip has a direct impact on the workspace of the body with an increase function. Fig. 3 shows workspace of the robot, when $L_1 = 550$ mm, $L_2 = 360$ mm, $L_3 = 150$ mm, $r = 300$ mm and $R = 630$ mm.

Same analyses also apply to study the workspace of the robot body when it employs three legs to attach on a wall. An example situation was chosen for the analyses when legs 1, 3 and 5 are adhering on the wall, while legs 2, 4 and 6 are lift up. The constraint equation in this situation can be written as

$$F_1(x, y, z, \alpha) = \begin{bmatrix} f_1 \\ f_3 \\ f_5 \end{bmatrix} . \tag{19}$$

The workspace of robot body is expressed as

$$W_{R1} = \left\{ (x, y, z, \alpha) \middle| F_1(x, y, z, \alpha) = 0 \right\} \tag{20}$$

where 0 is a 6x1 matrix. Equation $F_1(x, y, z, \alpha)$ is the constraint equation of the geometric center C of the body.

Same as the six-leg adhering situation, the range of the spherical center coordinate as well as the workspace of the

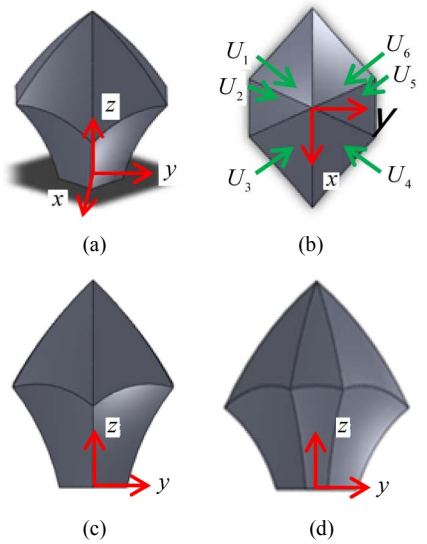

Fig. 3. The workspace of the robot using six legs to adhere on the wall: (a) Illustrative view; (b) vertical view; (c) front view; (d) left view.

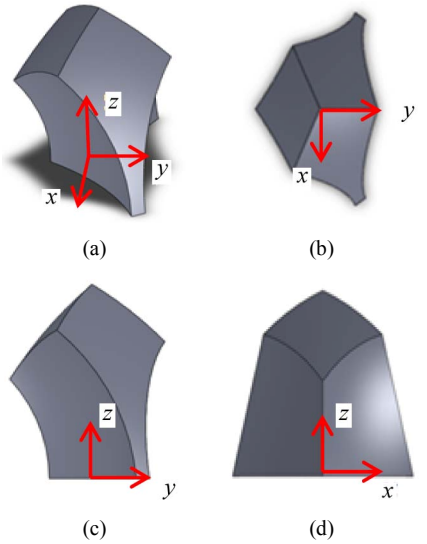

Fig. 4. The workspace of robot using legs 1,3 and 5 to adhere on the wall: (a) Illustrative view; (b) vertical view; (c) front view; (d) left view.

robot body increases with L_1, L_2 and L_3, showing that the length of the calf, thigh and hip has a direct impact on the workspace of the body with an increase function. Fig. 4 illustrates workspace of the robot when $L_1 = 550$ mm, $L_2 = 360$ mm, $L_3 = 150$ mm, $r = 300$ mm and $R = 630$ mm, with legs 1, 3 and 5 attaching on the wall.

By comparing Figs. 3 and 4, it can be seen that the workspace when the robot adheres on the wall with six legs is smaller than that with three legs. If A is the workspace of the attachment situation with six legs and B is that with three legs, then $A \subseteq B$.

Since each leg of the robot consists of three parts of the calf, thigh and hip, we studied the influence of the length of these three parts on the range of the workspace. When six legs are adhering on the wall, we define $U_i (i = 1, 2, 3, 4, 5, 6)$ as a curved surface, as shown in Fig. 4. When L_2 and L_3 are constant values, and L_1 become $L_1 + \Delta L_1$, $F_{1i}(x, y, z) = 0$ are the surface equation of U_i. When L_1 and L_3 are constant values, L_2 become $L_2 + \Delta L_2$, $F_{2i}(x, y, z) = 0$ are the surface equation of U_i. When L_1 and L_2 are constant values, and L_3 grows to $L_3 + \Delta L_3$, $F_{3i}(x, y, z) = 0$ are the surface equation of U_i. If $\Delta L_1 = \Delta L_2 = \Delta L_3$, it can be seen by the Eq. (12) that variation range of b_i and v_i are equal; by the Eq. (16) that the change range of center and the radius of each equation in Eq. (18) is equal. Therefore, we can conclude that $F_{1i} = F_{2i} = F_{3i}$, indicating that the influence of length change of the calf, thigh and hip on U_i is the same. With regard to three legs of robot absorb on the wall, the same conclusion can be obtained. Through the above analysis, from the point of view of kinematic, the length change of the calf, thigh and hip have same effects on the workspaces, respectively.

4. Singularity analysis

The initial configuration of the robot is shown in Fig. 2. When the robot walks with triangle gait using three legs to adhere on a wall and three legs swing, it can be seen as a 3SRRR parallel mechanism. Moreover, it can be regarded as a 6SRRR parallel mechanism during the posing mode with six legs attaching on the wall. When the robot cleans glass curtain walls, the robot body is required to be parallel to the wall. Thus, researches of singularity are limited to the body postures that are parallel to the vertical wall. Next, singularities of two kinds of configurations are introduced in this section.

Following the above analysis, here, we select the four parameters x, y, z and α as independent variables of $F(x, y, z, \alpha)$ in Eq. (16). Therefore, we define a new simple Jacobian matrix of equation $F(x, y, z, \alpha)$, it can be expressed as

$$J = \frac{\partial F(x, y, z, \alpha)}{\partial (x, y, z, \alpha)} = \begin{bmatrix} k_1 & m_1 & s_1 & t_1 \\ k_2 & m_2 & s_2 & t_2 \\ k_3 & m_3 & s_3 & t_3 \\ k_4 & m_4 & s_4 & t_4 \\ k_5 & m_5 & s_5 & t_5 \\ k_6 & m_6 & s_6 & t_6 \end{bmatrix} \tag{21}$$

where

$$\begin{cases} k_1 = 2\left(x + \dfrac{\sqrt{2}}{2} ru + \dfrac{\sqrt{2}}{2} R - b_1 \right) \\ m_1 = 2\left(y - \dfrac{\sqrt{2}}{2} rn + \dfrac{\sqrt{2}}{2} R - v_1 \right) \\ s_1 = 2(z - h_1) \\ t_1 = \sqrt{2} rn \left(x + \dfrac{\sqrt{2}}{2} ru + \dfrac{\sqrt{2}}{2} R - b_1 \right) \\ \quad + \sqrt{2} ru \left(y - \dfrac{\sqrt{2}}{2} rn + \dfrac{\sqrt{2}}{2} R - v_1 \right) \end{cases} \tag{22}$$

$$\begin{cases} k_2 = 2\left(x + rs\alpha - b_2\right) \\ m_1 = 2\left(y - rc\alpha + R - v_2\right) \\ s_2 = 2(z - h_2) \\ t_1 = 2r\left(x + rs\alpha - b_2\right)c\alpha \\ \quad + 2r\left(y - rc\alpha + R - v_2\right)s\alpha \end{cases} \tag{23}$$

$$\begin{cases} k_3 = 2\left(x + \frac{\sqrt{2}}{2}rn - \frac{\sqrt{2}}{2}R - b_3\right) \\ m_3 = 2\left(y + \frac{\sqrt{2}}{2}ru + \frac{\sqrt{2}}{2}R - v_3\right) \\ s_3 = 2(z - h_3) \\ t_3 = -\sqrt{2}ru\left(x + \frac{\sqrt{2}}{2}rn - \frac{\sqrt{2}}{2}R - b_3\right) \\ \quad + \sqrt{2}rn\left(y + \frac{\sqrt{2}}{2}ru + \frac{\sqrt{2}}{2}R - v_3\right) \end{cases} \tag{24}$$

$$\begin{cases} k_4 = 2\left(x - \frac{\sqrt{2}}{2}ru - \frac{\sqrt{2}}{2}R - b_4\right) \\ m_4 = 2\left(y + \frac{\sqrt{2}}{2}rn - \frac{\sqrt{2}}{2}R + v_4\right) \\ s_4 = 2(z - h_4) \\ t_4 = -\sqrt{2}rn\left(x - \frac{\sqrt{2}}{2}ru - \frac{\sqrt{2}}{2}R - b_4\right) \\ \quad - \sqrt{2}ru\left(y + \frac{\sqrt{2}}{2}rn - \frac{\sqrt{2}}{2}R + v_4\right) \end{cases} \tag{25}$$

$$\begin{cases} k_5 = 2\left(x - rs\alpha - b_5\right) \\ m_5 = 2\left(y + rc\alpha - R + v_5\right) \\ s_5 = 2(z - h_5) \\ t_5 = -2r(x - rs\alpha - b_5)c\alpha \\ \quad - 2r(y + rc\alpha - R + v_5)s\alpha \end{cases} \tag{26}$$

$$\begin{cases} k_6 = 2\left(x - \frac{\sqrt{2}}{2}rn + \frac{\sqrt{2}}{2}R - b_6\right) \\ m_6 = 2\left(y - \frac{\sqrt{2}}{2}ru - \frac{\sqrt{2}}{2}R + v_6\right) \\ s_6 = 2(z - h_6) \\ t_6 = \sqrt{2}ru\left(x - \frac{\sqrt{2}}{2}rn + \frac{\sqrt{2}}{2}R - b_6\right) \\ \quad - \sqrt{2}rn\left(y - \frac{\sqrt{2}}{2}ru - \frac{\sqrt{2}}{2}R + v_6\right). \end{cases} \tag{27}$$

Since the robot body is parallel to the wall, it can be obtained

$$z = h_i \tag{28}$$

That is

$$s_i = 0 \tag{29}$$

where $i = 1, 2, 3, 4, 5, 6$.

Substituting Eq. (29) into Eq. (21), the following equation is gained

$$R(J) = 3 \tag{30}$$

where $R(J)$ expresses the rank of matrix J.

The matrix J is not a full rank matrix, which indicates that the robot is on the singular configuration when it uses six feet to attach on the wall. The new Jacobian matrix greatly simplifies the solution of the Jacobian matrix of robots, making the singularity analysis of the parallel mechanism become simple.

Next, when the robot adheres on the wall with three legs, it still keeps the body parallel to the wall surface. If the matrix J_1 is the Jacobian matrix of $F_1(x, y, z, \alpha)$ in Eq. (19), it can be expressed as

$$\begin{aligned} J_1 = \frac{\partial F_1(x, y, z, \alpha)}{\partial(x, y, z, \alpha)} &= \begin{bmatrix} k_1 & m_1 & s_1 & t_1 \\ k_3 & m_3 & s_3 & t_3 \\ k_5 & m_5 & s_5 & t_5 \end{bmatrix} \\ &= \begin{bmatrix} k_1 & m_1 & 0 & t_1 \\ k_3 & m_3 & 0 & t_3 \\ k_5 & m_5 & 0 & t_5 \end{bmatrix}. \end{aligned} \tag{31}$$

Supposing that

$$J_2 = \begin{bmatrix} k_1 & m_1 & t_1 \\ k_3 & m_3 & t_3 \\ k_5 & m_5 & t_5 \end{bmatrix}. \tag{32}$$

Then

$$rank(J_1) = rank(J_2). \tag{33}$$

Since they have the same ranks, the singularity condition of matrix J_1 can be calculated in the following form

$$\det(J_2) = 0. \tag{34}$$

In order to simplify the calculation of determinant of J_2, it is supposed that $\alpha = 0$ rad, $L_1 = 550$ mm, $L_2 = 300$ mm, $L_3 = 150$ mm, $r = 300$ mm and $R = 630$ mm and $z \in$ [519 mm, 892 mm] without loss of generality. The determinant of J_2 can be obtained by varying platform parameters x from -100 mm to 100 mm and y from -100 mm to 100 mm, as shown in Fig. 5.

It is shown in Fig. 5 that the value of determinant of J_2 continuously changes from negative to positive. When the determinant of J_2 is equal to zero, the mechanism reaches a singular configuration. Fig. 6(a) offers a clear view of the

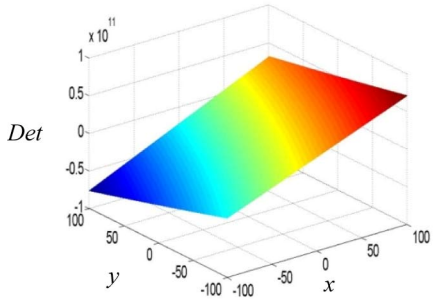

Fig. 5. The determinant of J_2 with the change of parameters x and y.

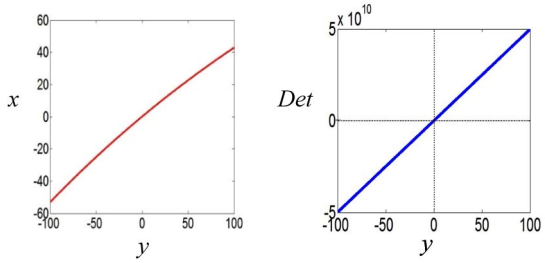

Fig. 6. (a) The functional relation of the parameter x with y; (b) the functional relation of the determinant of J_2 with parameter x.

singular configuration on the $x-y$ plane when the determinant of $J_2=0$. The curve is the singular position of the mechanism. If $y=0$, the functional image of the determinant of J_2 with x is a straight line, as shown in Fig. 6(b). It is shown in Fig. 6(b) that when both x and y are zero, the determinant of J_2 is also zero, explaining that positions of $x=y=0$ and $z\in[519\text{ mm}, 892\text{ mm}]$ are singular configurations of the mechanism.

Through the analysis, when the robot walks on the wall with the triangular gait, the robot will not be singularity. By introducing new Jacobian matrix, it greatly simplifies the calculation of Jacobian matrix of robot. Meanwhile, obtaining the singular configurations of the robot adhere on the vertical wall with six or three feet.

5. Experiments

In the above, the singularity of robot is analyzed by new Jacobian matrix. It is obtained that the robot is not singular when the robot walks on the wall with the triangular gait. Next, through experiments to show that the robot walks on the wall with the triangular gait, the robot will not be singularity. The structural parameters of robot are $L_1=550$ mm, $L_2=360$ mm, $L_3=150$ mm, $r=300$ mm, and $R=630$ mm. According to the structural parameters of robot, the suction cup which is produced by Japanese SMC company is selected, of which the model is ZP2-250HTN. According to torque requirements of each joint of the robot, the motors and the retarders produced by Shenzhen Techservo Co. Ltd. in China are selected. The models of the motors and the retarders are shown in Table 1.

Table 1. The model of motors and retarders of the wall climbing hexapod robot.

Joint	Motor	Retarder-A	Retarder-B
Joint 1	ST8N40P10V2E	S042L3-100	RAD-60-2
Joint 2	ST8N60P20V2E	S042L3-100	RAD-60-2
Joint 3	ST8N40P10V4E	S042L3-100	RAD-60-2

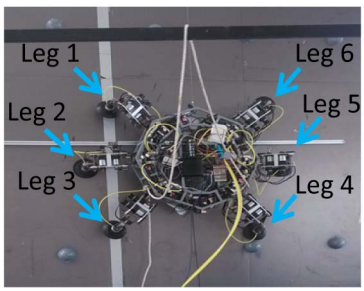

Fig. 7. The prototype of the wall climbing hexapod robot.

The connection mode of joint $i(i=1, 2, 3)$ is that motor series Retarder-A and series Retarder-B. The motors and retarders are selected of Joints 1, 2 and 3 of each leg which are corresponding to the same. The prototype of the wall climbing hexapod robot is shown as Fig. 7, the total mass of the robot is 72 kg.

For simplify the verification of singular configuration of the robot, and without losing generality, we select the most commonly used triangular gait of the hexapod robot to verify the singularity of the robot. Here, the robot which selects the mixed triangular gait [30] walks on the vertical wall, as shown in Fig. 8. "•" indicates supporting leg, "◦" means swinging leg, and "→" expresses the walking direction of the robot. In the Fig. 8, Stage ① denotes the initial standing configuration, Stages ② and ③ are the movement stages in which three legs lifting and swinging, and other three legs supporting and kicking, so that the robot body to move forward. Stage ④ represents one switching phase in which the supporting legs do not lift and the swinging legs contact the ground. Stages ⑤ and ⑥ are the movement stages in which the swinging legs in previous movement stage become supporting legs, and the supporting legs in previous movement stage become swinging legs. Stage ⑦ is one switching stage, similar to the Stage ④. Stages ⑧ and ⑨ are one movement stage in which the supporting legs and swinging legs change each other. Stages ①–③ are the starting gait of robot, and Stages ④–⑨ are a gait cycle of robot walking continuously.

If the robot is in singular configuration, then the motor current of the robot will suddenly become huge and tend to infinity. In Sec. 4, obtaining that the positions of $x=y=0$ and $z\in[519\text{ mm}, 892\text{ mm}]$ are singular configurations of robot, other configurations are not singular. If the robot walks with mixed triangular gait, the projection of geometric center of body does not coincide with the geometric center of adherence site of three supporting legs, thus, the robot does not have

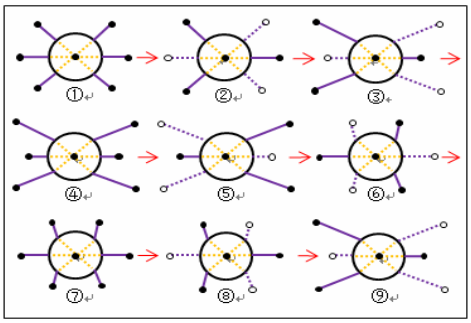

Fig. 8. Mixed triangular gait of the robot with horizontal direction.

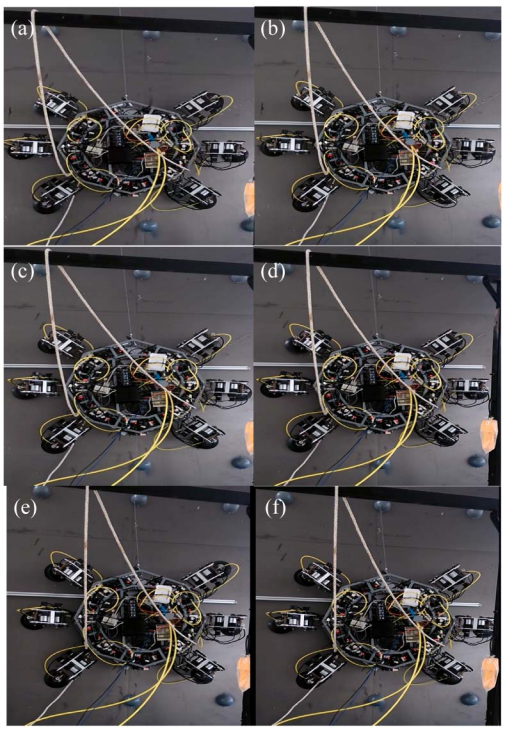

Fig. 9. The walking trajectory of the wall climbing hexapod robot walking on the vertical wall with horizontal direction to right by using the mixed triangular gait.

singular configurations with triangular gait. Assume that $J_{ij}(i=1, 2, 3, 4, 5, 6;\ j=1, 2, 3)$ is the motor current of the j th joint on the i th leg, the i th leg is marked in Fig. 7.

Next, the robot walks on the vertical wall with horizontal direction by using the mixed triangular gait, and the walking trajectory is shown in Fig. 9. By the experiments, obtaining that the relationship between the motor current $I_{i1}(i=1, 2, 3, 4, 5, 6)$ (A) and time t (s) is shown in Fig. 10, the relationship between the motor current $I_{i2}(i=1, 2, 3, 4, 5, 6)$ (A) and time t (s) is shown in Fig. 11, the relationship between the motor current $I_{i3}(i=1, 2, 3, 4, 5, 6)$ (A) and time t (s) is shown in Fig. 12.

By Fig. 10, it is obtained that the current $I_{i1}(i=1, 2, 3, 4, 5, 6)$ does not tend to infinity, the curve of the current change is smooth, and the difference between the maximum value and the minimum value of the current

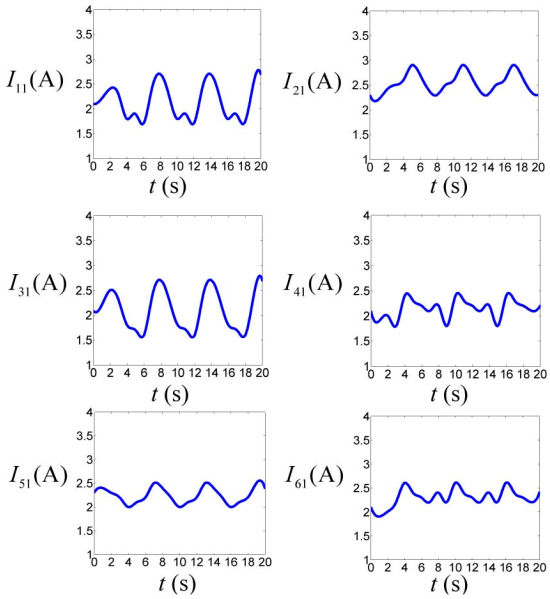

Fig. 10. The relationship between the current $I_{i1}(i=1, 2, 3, 4, 5, 6)$ (A) and time t (s) when robot walks on the vertical wall using mixed triangular gait.

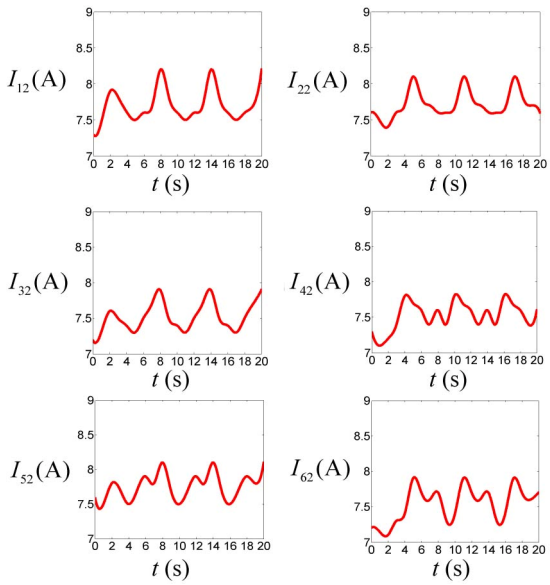

Fig. 11. The relationship between the current $I_{i2}(i=1, 2, 3, 4, 5, 6)$ (A) and time t (s) when robot walks on the vertical wall using mixed triangular gait.

$I_{i1}(i=1, 2, 3, 4, 5, 6)$ is 1.2 (A). So the 1 th joint of each leg of the robot does not occur singularity. By Fig. 11, it is obtained that the current $I_{i2}(i=1, 2, 3, 4, 5, 6)$ does not tend to infinity, the current is relatively stable, and the difference between the maximum value and the minimum value of the current $I_{i2}(i=1, 2, 3, 4, 5, 6)$ is 0.9 (A). So the 2nd joint of each leg of the robot does not occur singularity. By Fig. 12, obtaining the current $I_{i3}(i=1, 2, 3, 4, 5, 6)$ does not tend to infinity, the current does not greatly fluctuate, and the difference between the maximum value and the minimum value of the cur-

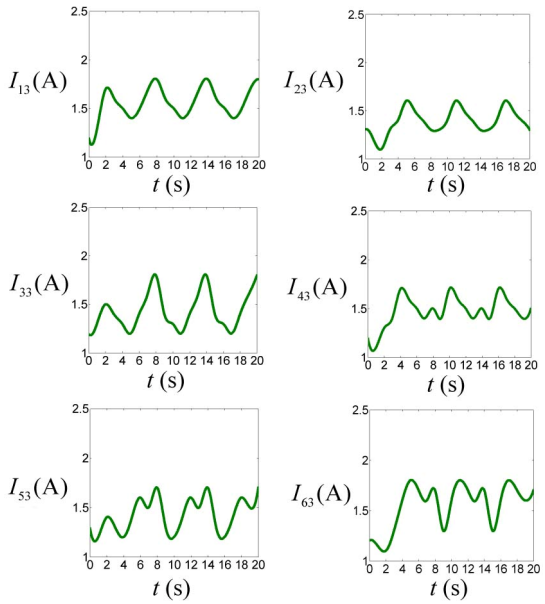

Fig. 12. The relationship between the current $I_{i3}(i=1, 2, 3, 4, 5, 6)$ (A) and time t (s) when robot walks on the vertical wall using mixed triangular gait.

rent $I_{i3}(i=1, 2, 3, 4, 5, 6)$ is 0.7 (A). So the 3rd joint of each leg of the robot does not occur singularity. Therefore, it is shown that the robot does not have singular configurations when robot is walking on the wall by using the mixed triangular gait. So the singularity analysis conclusion that the robot walks on the wall with the triangular gait, the robot will not be singularity in Sec. 4 is correct.

6. Discussions

In this paper, we mainly studied the mechanism of wall climbing hexapod robot by the screw theory and constraint equations from a theoretical point of view. However, in application, the weight to power ratio of its actuators is major indicator of designing robot. The robot has 18 motors, the total energy consumption of robot is large, so the energy optimization of robot should be considered, and selecting a more suitable motors in application. Meanwhile, the weight of the body frame is large, to make the legs of robot produce deformation, affecting the trajectory of robot. Thus, when the robot is walking and working in the actual environment, the influence of the structural deformation on control of the robot should be considered in future work. Moreover, the robot has 18 motors, each motor is likely to be involved in the motion at the same time, therefore, the coordinated control of motors should be considered in the future.

This paper discusses the DOF, workspace and singularity of the robot with six legs and three legs adhere on the wall. In a particular environment, the robot may walk with one-by-one gait, quadrupedal gait and five feet gait, so we can investigate their the DOF, workspace and singularities, respectively. Moreover, the Jacobian matrix of the parallel mechanism mainly reflects the relationship between active input variables and independent output variables, however, 18 motors of the robot are all likely to participate in the motion when the robot is walking, and provide torque. Therefore, each joint is likely to produce singularity on the robot body, so the singularity of the 18 motors can be discussed in the future.

At singular configurations, the kinematics, dynamics or stability of robot may instantaneous mutation, leading to the lost of the delivering ability for motion and power of the mechanical structures. Moreover, when the robot is near to the regions of singular configurations, the Jacobian matrix gets close to a reduced rank. The stiffness property, motion transfer performance and stability of mechanism may perform unexpectedly. Therefore, the robot should be controlled to avoid the occurrence of these singular configurations and be kept away from regions close to the singular configurations to ensure normal operations.

7. Conclusions

In this paper, we investigate the DOF, workspace and singularity of a wall climbing hexapod robot. The robot possesses two kinds of configurations. The robot is regarded as a parallel mechanism when it attaches on a wall with six feet or three feet. The DOF analysis by screw theory shows that both of these two configurations of the robot have 6-DOF coupling with three translations and three rotations. The robot body therefore can realize flexible motions of 6-DOF. Meanwhile, no matter where the robot adheres on a wall with six or three feet, the robot body can achieve the flexible motions with 6-DOF.

After that, the workspaces of these two kinds of configurations of the robot are expressed through constraint equations. Meanwhile, by the further mathematical deduction indicates that the influence of the length of the calf, thigh and hip of the robot on $U_i(i=1, 2, 3, 4, 5, 6)$ is the same. Furthermore, since singularity affects the continuity of the motion of a parallel robot, the singular conditions of these two configurations are analyzed with the rank and determinant of a new simple Jacobian matrix. The singular configurations of these two configurations are obtained. Thus, the robot is needed to work away from the singular configurations and regions close to them to ensure normal performances. Finally, by experiments to show that the singularity analysis of robot is correct. The analysis method of the DOF, workspace and singularity is proposed in this paper can be used to study other robot systems and parallel mechanisms.

Acknowledgements

The work was supported by National Natural Science Foundation of China (Grant No. 51275360, 51538009 and 51605334), Excellent Technology Leadership Program of Shanghai (Grant No. 15XD1525000) and Shanghai Sailing Program (Grant No. 17YF1420900). The authors would like

to express thanks to Jiangsu Greenhub Technology Co. Ltd., China, for its technical support.

Nomenclature

DOF : Degrees of freedom

Reference

[1] K. Nagaya, T. Yoshino, M. Katayama, I. Murakami and Y. Ando, Wireless piping inspection vehicle using magnetic adsorption force, *IEEE/ASME Transaction on Mechatronics*, 17 (3) (2012) 472-479.

[2] E. Sato, S. Iki, K. Yamanishi, H. Horibe and A. Matsumoto, Dismantlable adhesion properties of reactive acrylic copolymers resulting from cross-linking and gas evolution, *The Journal of Adhesion*, 7 (2016) 1-12.

[3] G. Lee, H. Kim, K. Seo, J. Kim, M. Sitti and T. Seo, Series of multilinked caterpillar track-type climbing robots, *Journal of Field Robotics*, 33 (6) (2016) 737-750.

[4] J. Jiang, Y. Zhang and S. Zhang, Implementation of glass-curtain-wall cleaning robot driven by double flexible rope, *Industrial Robot: An International Journal*, 41 (2014) 429-438.

[5] Y. Liu, H. Kim and T. Seo, Anyclimb: A new wall-climbing robotic platform for various curvatures, *IEEE/ASME Transaction on Mechatronics*, 21 (3) (2016) 1812-1821.

[6] Y. Liu, S. Sun, X. Wu and T. Mei, A wheeled wall-climbing robot with bio-inspired spine mechanisms, *Journal of Bionic Engineering*, 12 (1) (2015) 17-28.

[7] F. Xu, J. Shen, J. Hu and G. Jiang, A rough concrete wall-climbing robot based on grasping claws: Mechanical design,analysis and laboratory experiments, *International Journal of Advanced Robotic Systems*, 10 (2016) 1-10.

[8] S. Fujii et al., Ladder climbing control for limb mechanism robot "ASTERISK", *IEEE International Conference on Robotics and Automation,* Pasadena, USA (2008) 3052-3057.

[9] Z. Wang, X. Ding, A. Rovetta and A. Giusti, Mobility analysis of the typical gait of a radial symmetrical six-legged robot, *Mechatronics*, 21 (2011) 1133-1146.

[10] M. C. García-López, E. Gorrostieta-Hurtado, E. Vargas-Soto, J. M. Ramos-Arreguín, A. Sotomayor –Olmedo and J. C. Moya Morales, Kinematic analysis for trajectory generation in one leg of a hexapod robot, *Procedia Technology*, 3 (2012) 342 - 350.

[11] H. Zhang, Y. Liu, J. Zhao, J. Chen and J. Yan, Development of a bionic hexapod robot for walking on unstructured terrain, *Journal of Bionic Engineering*, 11 (2014) 176-187.

[12] Z. Deng, Y. Liu, L. Ding, H. Gao, H. Yu and Z. Liu, Motion planning and simulation verification of a hydraulic hexapod robot based on reducing energy/flow consumption, *Journal of Mechanical Science and Technology*, 29 (10) (2015) 4427-4436.

[13] D. Gan, J. Dai and D. G. Caldwell, Constraint based limb synthesis and mobility change aimed mechanism construction, *ASME/Journal of Mechanical Design*, 133 (5) (2011) 051001_1-051001_9.

[14] X. Kong and C. M. Gosselin, Type synthesis of 3 DOF spherical parallel manipulators based on screw theory, *ASME/Journal of Mechanical Design*, 126 (2004) 101-108.

[15] J. Dai, Z. Huang and H. Lipkin, Mobility of overconstrained parallel mechanisms, *ASME/Journal of Mechanical Design,* 128 (2006) 220-229.

[16] W. Bu, S. Yan, J Chen and X. An, Mobility analysis for parallel manipulators based on intersection of screw manifolds, *Journal of Mechanical Science and Technology*, 30 (9) (2016) 4345-4352.

[17] J. P. Merlet, Direct kinematics and assembly modes of parallel manipulators, *The International Journal of Robotics Research*, 2 (1992) 150-162.

[18] Z. Wang et al., A study on workspace, boundary workspace analysis and workspace positioning for parallel machine tools, *Mechanism and Machine Theory*, 5 (2001) 605-622.

[19] Z. Gao, G. Wei and J. Dai, Inverse kinematics and workspace analysis of the metamorphic hand, *Proc IMechE Part C: J. Mechanical Engineering Science* (2014) 1-11.

[20] M. Agheli and S. S. Nestinger, Closed-form solution for constant-orientation workspace and workspace-based design of radially symmetric hexapod robots, *Journal of Mechanisms and Robotics*, 6 (8) (2014) Doi: 10.1115/1.4026827.

[21] D. Szep, S. Stan and V. Csibi, Design, workspace analysis, and inverse kinematics problem of delta parallel robot, *Mechanika*, 17 (3) (2011) 296-299.

[22] R. Maldonado-Echegoyen, E. Castillo-Castaneda and M. A. Garcia-Murillo, Kinematic and deformation analyses of a translational parallel robot for drilling tasks, *Journal of Mechanical Science and Technology*, 29 (10) (2015) 4437-4443.

[23] C. Gosselin, Determination of the workspace of 6 DOF parallel manipulators, *Journal of Mechanical Design*, 3 (1990) 331-336.

[24] J. P. Merlet, Singular configurations of parallel manipulator and grassman geometry, *The International Journal of Robotics Research,* 5 (1989) 45-56.

[25] J. Gallardo-Alvarado et al., Kinematics of an asymmetrical three legged parallel manipulator by means of the screw theory, *Mechanism and Machine Theory*, 45 (2010) 1013-1023.

[26] D. Gan et al., Forward displacement analysis of a new 1CCC-5SPS Parallel mechanism using Grobner theory, *Proc IMechE Part C: J. Mechanical Engineering Science*, 223 (5) (2009) 1233-1241.

[27] S. Zarkandi, Kinematics and singularity analysis of a parallel manipulator with three rotational and one translational DOFs, *Mech. Based Des Struct. Mach.*, 39 (2011) 392-407.

[28] J. Zhao, Y. Fu, K. Zhou and Z. Feng, Mobility properties of a Schoenflies-type parallel manipulator, *Robotics and Computer Integrated Manufacturing*, 22 (2006) 124-133.

[29] D. Gan, J. Dai and D. Caldwell, *Constraint-screw system based synthesis of limb arrangement of the 3-PUP parallel mechanism*, J. Lenarcic and M. M. Stanisic (eds), Advances in robot kinematics: motion in man and machine, Dordrecht:

Springer, 8 (2010) 485-492.
[30] K. Xu and X. Ding, Typical gait analysis of a six-legged robot in the context of metamorphic mechanism theory, *Chinese Journal of Mechanical Engineering*, 4 (26) (2013) 771-783.

Bin He received the B.S. degree in engineering machinery from Jilin University, Changchun, China, in 1996, and the Ph.D. degree in mechanical and electronic control engineering from Zhejiang University, Hangzhou, China, in 2001. Between 2001 and 2003, he held postdoctoral research appointments with The State Key Labof Fluid Power Transmission and Control, Zhejiang University. He is currently a Professor in the Department of Control Science and Engineering, College of Electronics and Information Engineering, Tongji University, Shanghai, China. His current research interests include intelligent robot control, neural networks, biomimetic microrobots, image processing and fusion, wireless communication, and wireless networks. Dr. He is an Associate Editor of Neurocomputing.

Shoulin Xu is currently working toward the Ph.D. degree in the Deparment of Control Science and Engineering, College of Electronics and Information Engineering, Tongji University. His research interests include mechanism of parallel manipulator, dynamics and control of robotic systems.

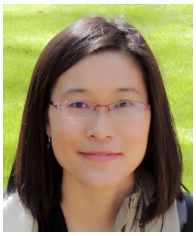

Yanmin Zhou is currently Assistant Professor in the Deparment of Control Science and Engineering, College of Electronics and Information Engineering, Tongji University. Her currently research interests include bionics, design and control of intelligent robot.

Zhipeng Wang received his Ph.D. degree from Tongji University in 2015. He is currently a post-doctoral in the School of Mechanical Engineering, Tongji University. His currently research interests include design, dynamics and control of robot.